

Microstructures and Properties of Electrodeposited Cu-Bi Composite Coatings

See Leng Tay^{1,2}, Xiaojin Wei¹, Weiwei Chen³, Caizhen Yao¹, Wei Gao^{1,*}

¹ Department of Chemical and Materials Engineering, the University of Auckland, Auckland 1142, New Zealand

² Department of Mechanical Engineering, University of Malaya, Kuala Lumpur, Malaysia

³ Department of Materials Science and Technology, Beijing Institute of Technology, Beijing, China

*E-mail: w.gao@auckland.ac.nz

Received: 11 October 2013 / Accepted: 29 January 2014 / Published: 2 March 2014

Copper-based composites are widely used in industry due to their desired properties. In this research, a Cu-Bi composite coating was successfully developed by electroplating. Current density was varied from 10-100 mA/cm² and deposition time was selected for preparing the samples. The properties of Cu-Bi coatings were characterised with comparison to pure Cu coating. Results showed that incorporation of Bi into Cu, refined the microstructure and improved the mechanical properties of coatings. The deposition current densities played an important role in producing good results. At a high current density of 100 mA/cm², porous microstructure was formed and caused inferior mechanical properties. However, the electrochemical or corrosion properties of the Cu-Bi composite were only slightly improved compared to the pure Cu coating.

Keywords: Cu-Bi composite, Electroplating, Microhardness, Strengthening Mechanism, Electrochemical Property

1. INTRODUCTION

Coating plays an important role in Materials Engineering as it can improve the mechanical properties and corrosion resistance, of surface and provide attractive appearance. A variety of coating technologies are used in industries [1]. One of the most common process is 'electroplating' [2], which was first introduced by an Italian Chemist, Brugnatelli in 1805 [3].

Composite coating is a type of coating consisting of two or more materials with different physical properties and/or chemical properties to obtain a desired properties to achieve the specific application [4]. This type of coating is often designed to have a second phases in a matrix [5]. The size and distribution of second phase particles can be controlled during the electro-deposition process [6].

Most of the recent composite coating studies were carried out by depositing insoluble metal oxide or ceramic particles as second phase into metal matrix such as Cu-Al₂O₃[7-9], Cu-Fe₃O₄ [10], Cu-MoS₂ [9], Cu-SiC [9, 11], Cu-SiO₂ [12], Cu-Si₃N₄ [13], Cu-TiO₂ [14], Cu-TiB₂ [15] and Cu-ZrB₂ [16]. However, few studies have focused on the deposition of two insoluble metals. In this research, a novel method called ionic co-discharge process is introduced to deposit Bi into Cu. Based on the phase diagram, Cu and Bi do not form any solid solution or intermetallic phase [17]. Cu-Bi composite coatings can be deposited at room temperature via a simple two electrode electroplating process as reported in our previous study [18]. The work studies the effect of deposition processing and Bi composition on the coating microstructure, phase structure, mechanical properties and electrochemical properties.

2. EXPERIMENTAL PROCEDURES

Two groups of samples were prepared: pure Cu coated and Cu-Bi coated samples. Pure Cu sheets (> 99.9% Cu) were used as the substrate. Before electroplating, pre-treatment of Cu substrate was carried out by alkaline cleaning in an alkaline solution containing 50 g/L NaOH and 10 g/L sodium carbonate decahydrate (Na₂CO₃·10H₂O) solution at 60 °C for 10 min. The substrate was then anodised in 20 g/L citric acid and 60 g/L ammonium citrate for 20 s at 1.1 mA/cm² and at ambient temperature.

A two-electrode system was used for the deposition of Cu and Cu-Bi. For Cu deposition, the electrolyte contained 110 g/L K₄P₂O₇, 40 g/L CuSO₄·5H₂O and 10 g/L Na₂HPO₄. The solution used for Bi electroplating contained 0.2 M Bi(NO₃)₃·5H₂O, 0.2 M tartaric acid and 2.5 M KOH. The pH was maintained at 12 by adjusting with NaOH solution. 3 ml Bi bath solution was added into 70 ml Cu electrolyte in the Cu-Bi electroplating. In order to obtain coatings with similar thickness for comparison purposes, deposition times of 30, 20 and 10 min were used for current densities of 10, 50 and 100 mA/cm², respectively.

The morphology of coatings and the content of Bi in Cu-Bi coatings were measured by scanning electron microscope (SEM) with an energy dispersion spectroscopy (EDS) attachment. The phase structure and crystallite size of the coatings were determined by using X-ray diffraction (XRD). The hardness of coatings was measured by using microhardness tester (Leco M400) with a Vickers diamond indenter. The applied load was 50 gf with a holding time of 10 s. At least 5 measurements under the same conditions were conducted, and the average value was calculated as the microhardness (HV). The wear property of the coatings was conducted by using a NANOVEA tribometer where a ceramic ball of 6 mm in diameter acted as friction counterpart. The test was conducted with a load of 1 N and sliding speed of 100 rpm at room temperature with a relative humidity of ~50%. The wear track was measured under an optical microscope. The volume loss was also calculated by equation (1):

$$\text{Volume loss, } V_{\text{loss}} = A_L L = L \left[r^2 \sin^{-1} \left(\frac{d}{2r} \right) - \frac{d}{4} \sqrt{4r^2 - d^2} \right] \quad (1)$$

where L is the length of the wear track (in mm), r is the radius of the ball used for wear testing (3 mm), and d is the wear track width (in mm).

The corrosion test was assessed by Tafel plot in 3.5 wt. % NaCl solution at room temperature with electrochemical workstation (CHI604D). A conventional three-electrode cell was used in the electrochemical testing. The sample acts as working electrode, a platinum plate as counter electrode and saturated calomel electrode (SCE) as a reference electrode. The exposure area was 10 mm × 10 mm and the rest area was sealed by silicone rubber. The potentiodynamic polarization curve were measured in a range of ±0.3 V from the open circuit potential (OCP) with a scan rate of 1 mV/s.

3. RESULTS AND DISCUSSION

3.1 Phase Structure and Orientation

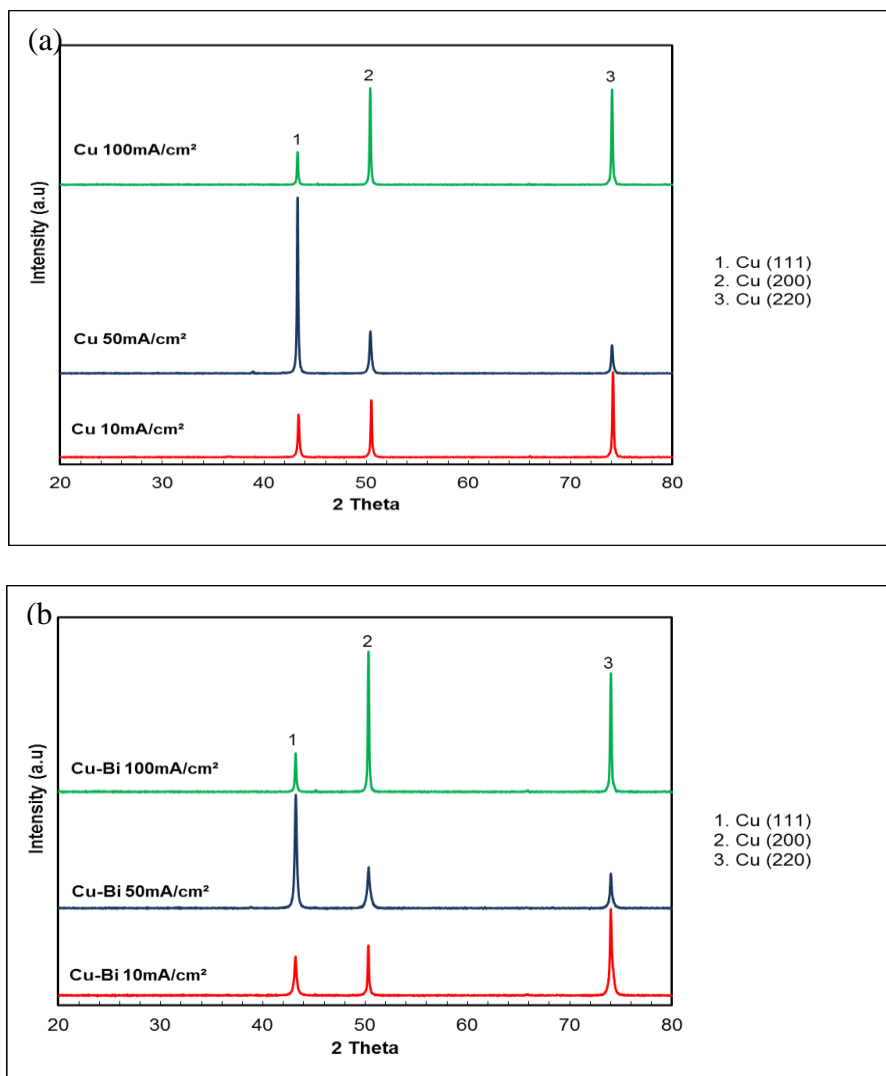


Figure 1. XRD patterns of the (a) Cu and (b) Cu-Bi electrodeposition.

Fig. 1 shows the XRD patterns of Cu and Cu-Bi coatings. Cu and Cu-Bi layers were deposited at 10, 50 and 100 mA/cm² for 30, 20 and 10 min, respectively.

Three predominant peaks were shown in these coatings: Cu (111), Cu (200) and Cu (220). No crystalline Bi peak was detected by the XRD due to the low concentration of Bi incorporated in Cu coating.

The crystallite size of Cu was calculated from the prominent peak via Scherrer's formula as shown in Table 1. Cu-Bi coatings showed a smaller grain size at all current densities compared to the Cu coatings. The crystallite size decreased with increasing current density up to 50 mA/cm², and increased at the higher current density.

Table 1. Crystallite size calculation from XRD patterns.

Coating	Crystallite size (nm)		
	10 mA/cm ²	50 mA/cm ²	100 mA/cm ²
Cu	63.5±1.1	48.1±7.7	66.5±1.9
Cu-Bi	43.3±8.6	35.4±3.7	61.3±4.3

3.2 Microstructure Characterization

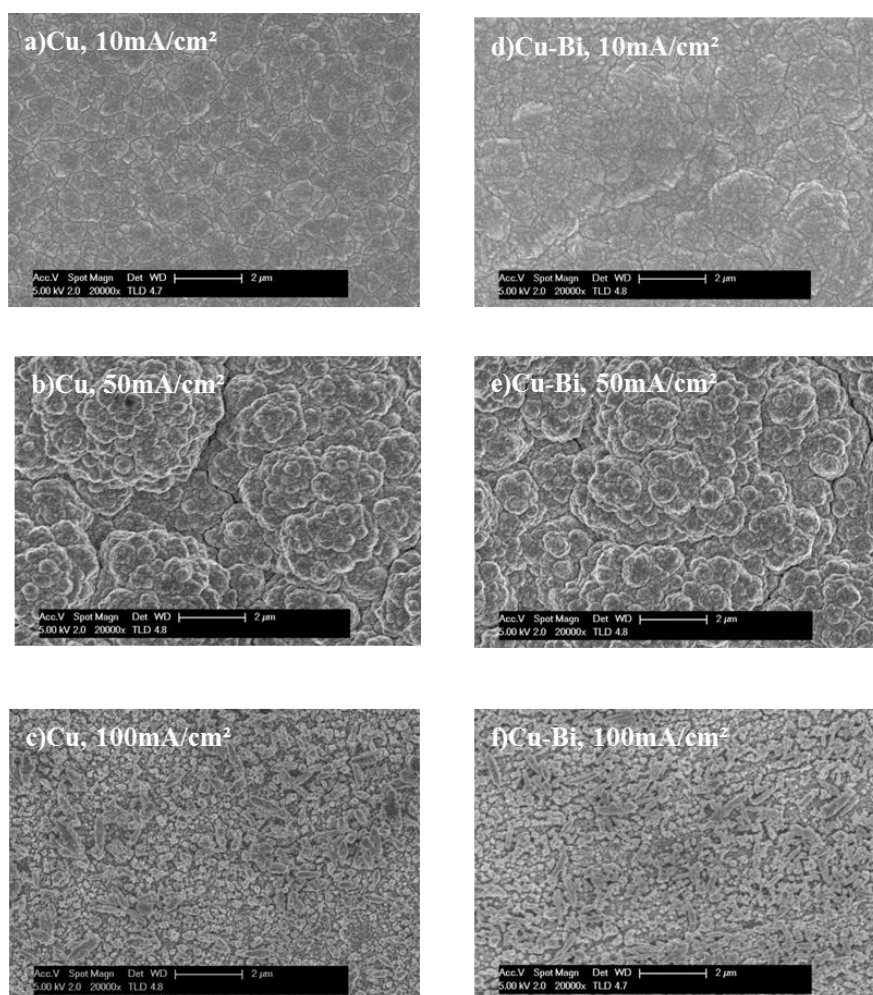


Figure 2. Top morphology of Cu and Cu-Bi electrodeposition on Cu substrate with variety of current densities.

The surface morphology of the Cu and Cu-Bi coatings at different current densities are shown in Fig. 2. The grain structure of the Cu and Cu-Bi composite coatings were round shaped and became finer at 50 mA/cm^2 . However, the morphology changed to the mixture of fine granular shape and elongated granular shape at 100 mA/cm^2 , consisting with the grain size calculation in Table 1.

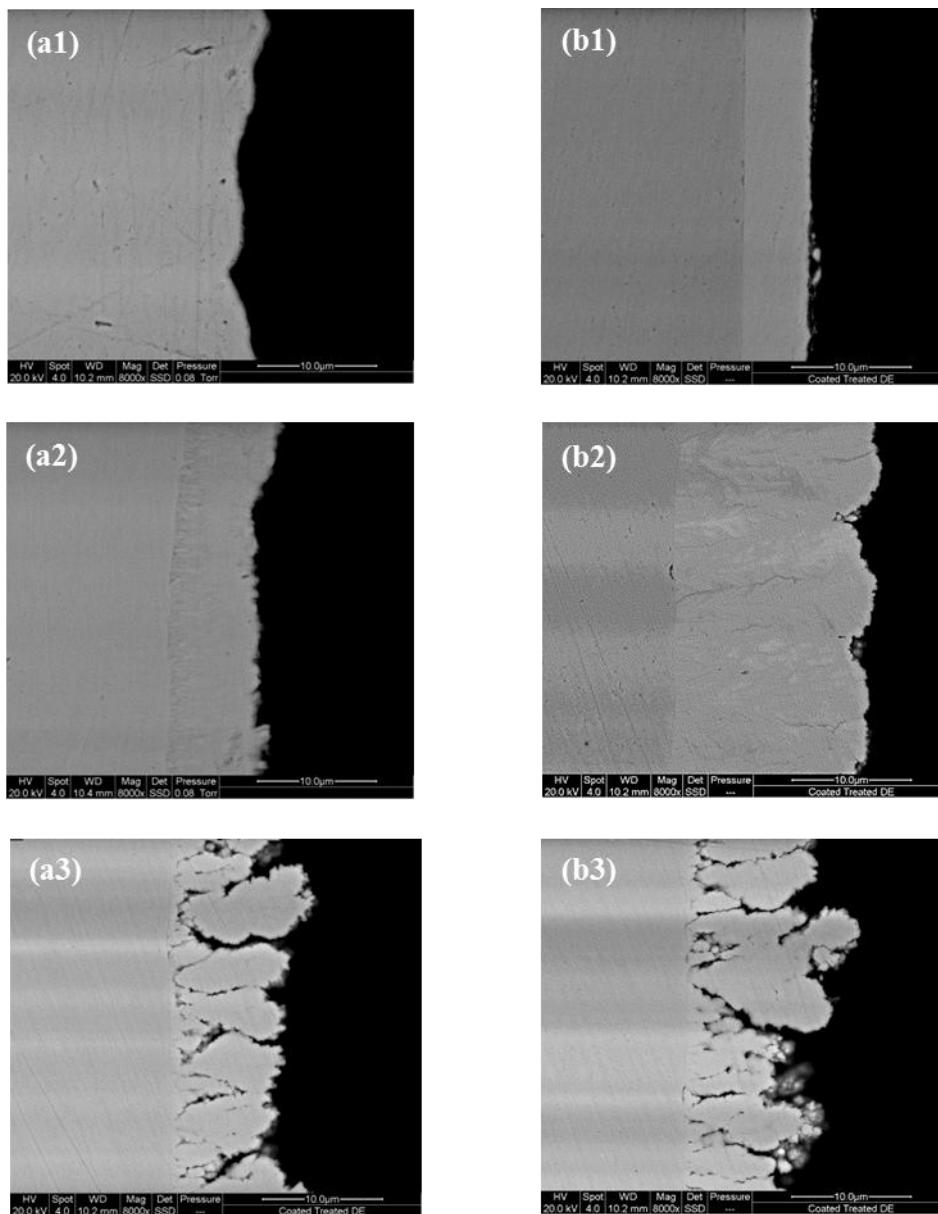


Figure 3. Cross-sectional morphologies of Cu and Cu-Bi coatings: (a1, b1) 10 mA/cm^2 for 30 min, (a2, b2) 50 mA/cm^2 for 20 min, and (a3, b3) 100 mA/cm^2 for 10 min. (a1, a2, a3) and (b1, b2, b3) are Cu and Cu-Bi coatings, respectively.

Fig.3 shows SEM micrographs of the cross-sectional Cu and Cu-Bi depositions at different current densities. Generally, Cu-Bi has a compact coating compared to the Cu coating at lower current density. At the high current density of 100 mA/cm^2 , both deposition were porous. Besides that, incorporation of Bi into Cu enhanced the deposition rate at lower current density. The thickness of the

Cu-Bi deposition was much thicker compared to the pure Cu coating. The thickness of Cu-Bi composite coating at 10, 50 and 100 mA/cm² were 5.5±0.1 μm, 16.0±0.2 μm, 9.1 ±1.4 μm, compared to the thickness of Cu coatings at 10, 50 and 100 mA/cm² of 3.7±0.6 μm, 7.3±0.4 μm and 8.6±1.2 μm, respectively.

3.3 Chemical Analysis

The composition of the Bi in the composite coatings was measured by EDS as shown in Fig. 4. Fig. 5 shows the content of the Bi deposited into Cu matrix, which decreased with increasing current density. This might be due to the shorter deposition time at higher current density.

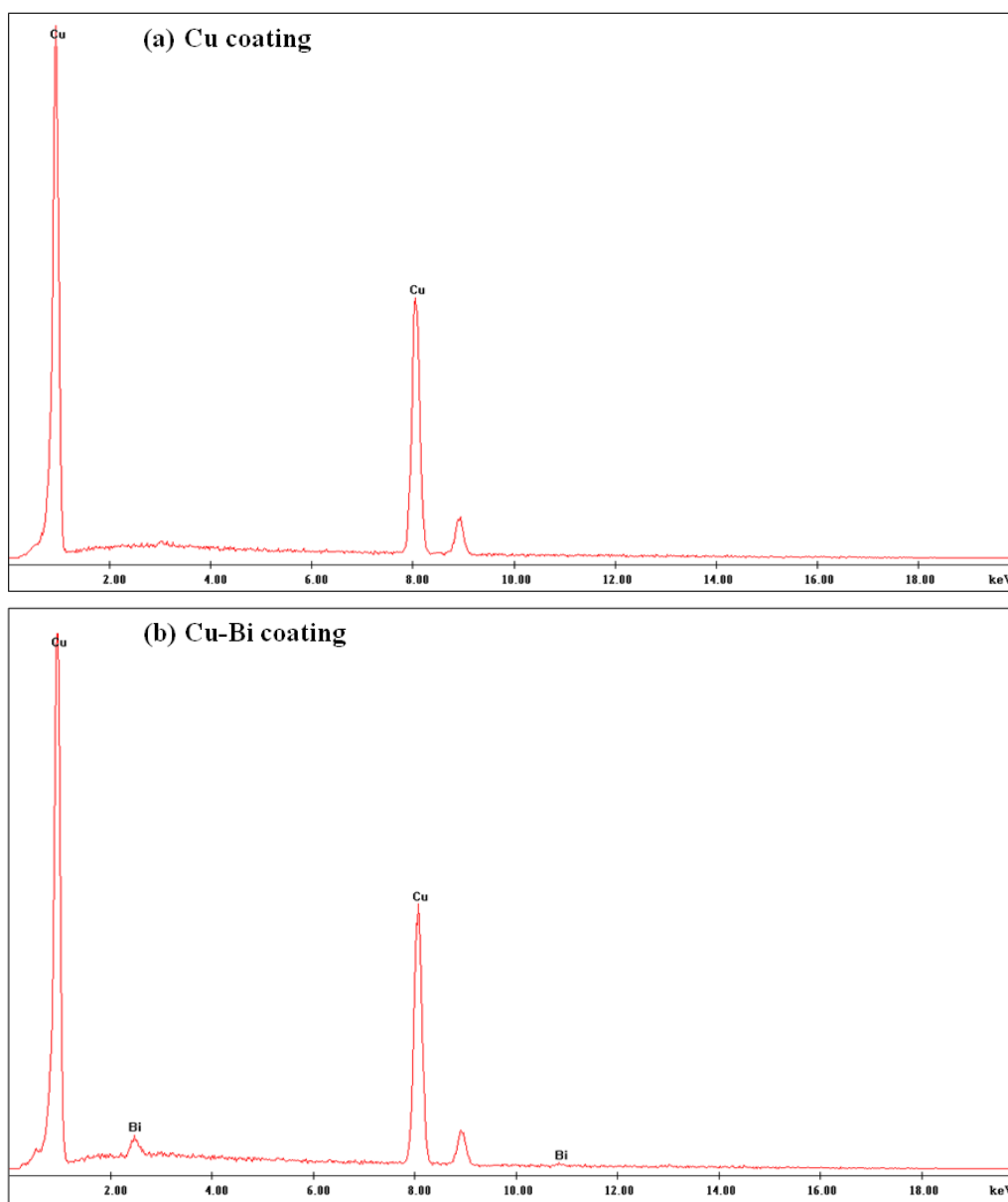


Figure 4. EDS spectrum of (a) Cu coating; (b) Cu-Bi coating at 10 mA/cm²

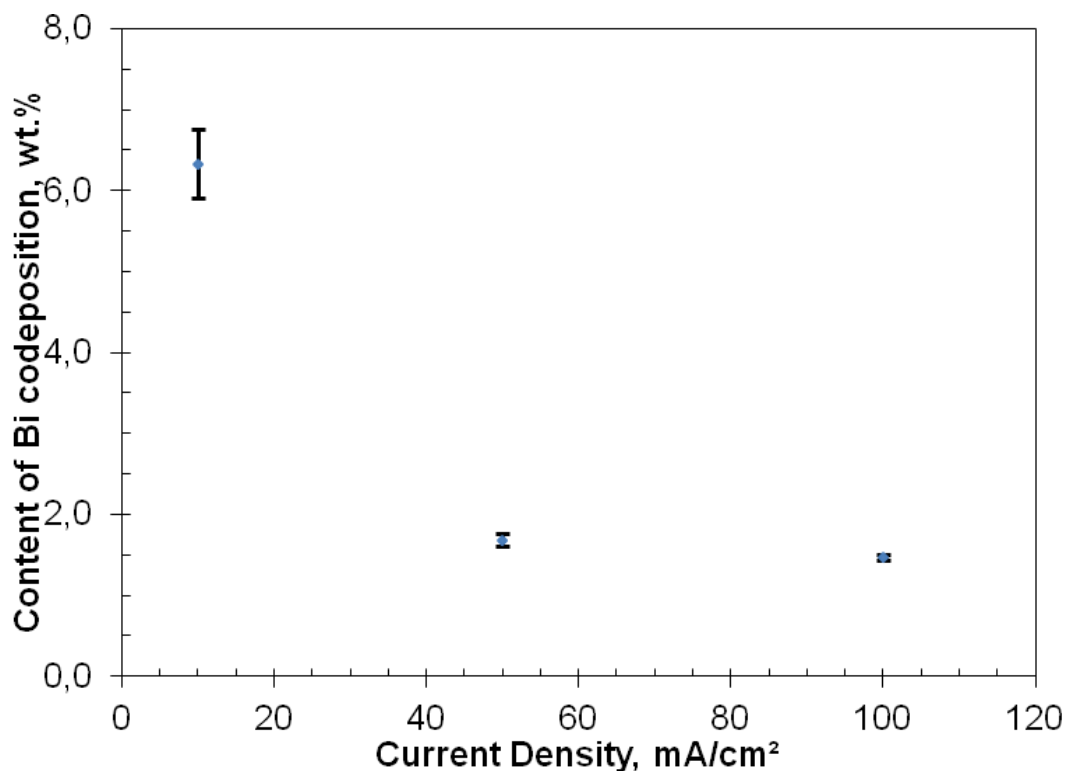


Figure 5. Content of Bi codeposition into Cu-Bi electrodeposition.

3.4 Mechanical Properties

3.4a Microhardness

The microhardness of coatings is shown in Fig. 6. Cu-Bi coating had higher microhardness compared to pure Cu coating at all current densities. It increased with current density up to 50 mA/cm², and then decreased 100 mA/cm².

Second phase-strengthening and particle-dispersion strengthening are two mechanisms to improve the mechanical strength of metals. Particle-strengthening was not considered in this case due to it only apply for the incorporation of the second phase with the volume percentage more than 20% [19]. Second phase strengthening follows the Orowan mechanism might be applied in this research due to the hardness value of the Cu composite was higher compare to pure Cu coating at entire current densities. Incorporation of Bi into Cu matrix can hinder the dislocation motion and thus enhanced the hardness [20]. Grain-refining is another mechanism as shown in Table 2. The microhardness value was affected by the crystallite size. The lower of crystallite size, the higher microhardness value was obtained. Lekka *et al.* [11] also reported that the microhardness of Cu coating was enhanced with the incorporation of micro and nano SiC particles into Cu matrix.

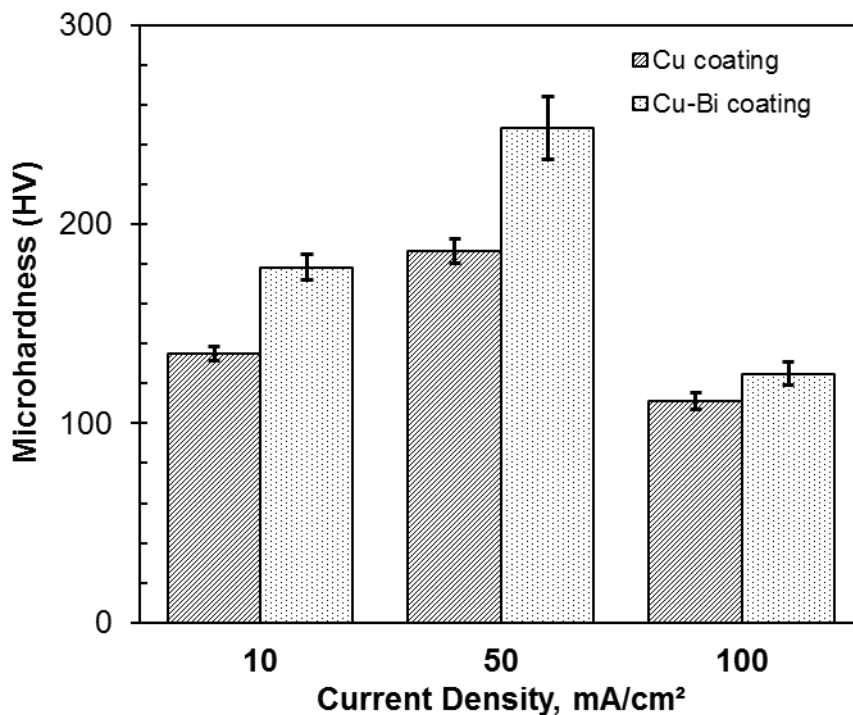


Figure 6. Microhardness value of Cu and Cu-Bi coating at different current density.

3.4b Wear Testing

Fig. 7 shows the volume loss and wear rate of the coatings deposited at different current density. Result revealed that Cu-Bi had a lower volume loss compared to the pure Cu coating, indicating that Cu-Bi had a better wear resistance than pure Cu coating. The width of wear tracks of Cu-Bi composite coating was much narrower compared to that on Cu coating as shown in Fig.8. This is believed due to the strengthening effect of Cu-Bi coatings. The finer microstructure of addition Bi might cause less of the volume loss and less groove were given rise to. This results had a similar found out with addition Al in Zn electroplating [21].

It can also be seen that the volume loss generally increases with the current density for both coatings. However, Cu coating showed the highest volume loss at 50mA/cm² because of the very porous microstructure (Fig. 3 a2).

The trend of wear loss increase of Cu-Bi coatings may also relate to the Bi content in the coating as shown in Fig. 5. The higher Bi content in the coating showed the lower volume loss, and thus provides a better wear resistance. Both Cu and Cu-Bi coating deposited at high current density had a similar volume loss ($\sim 0.77 \times 10^{-3} \text{ mm}^3$), corresponding to the same porous microstructure as shown in Fig. 3 (a3 and b3).

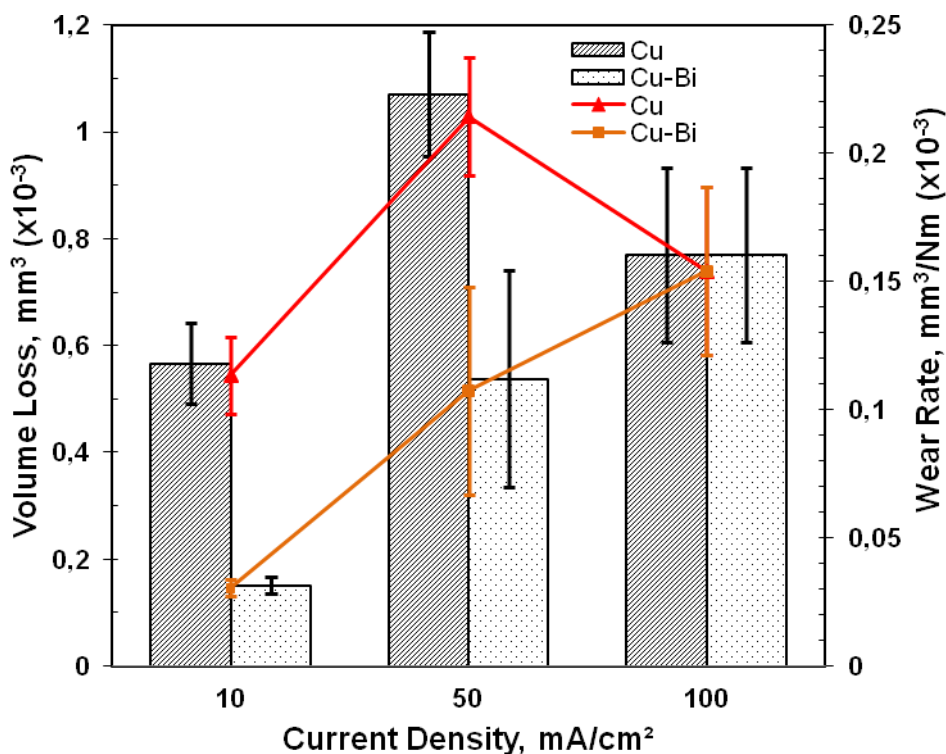


Figure 7. Volume loss and wear rate of Cu and Cu-Bi coating at different current density.

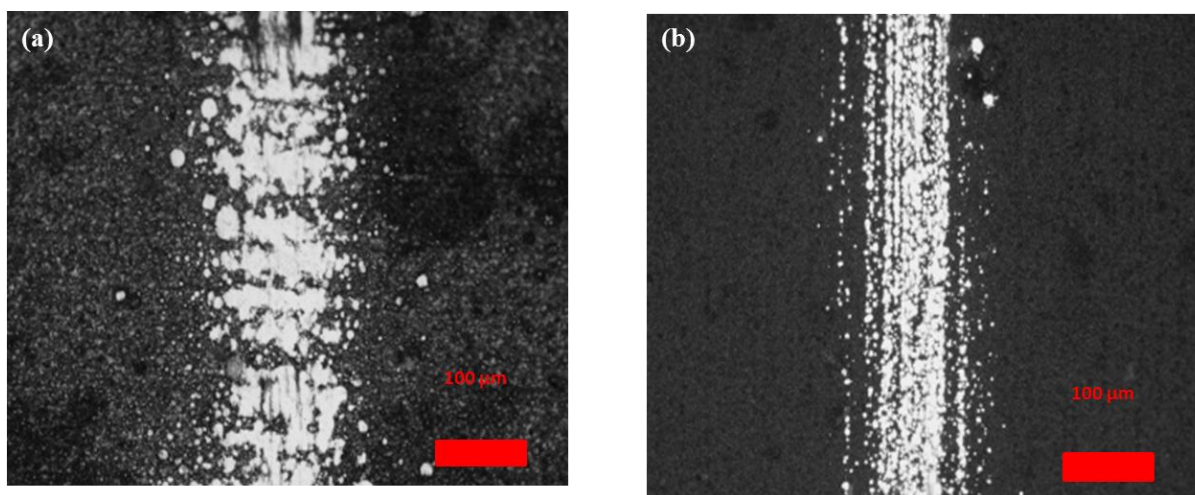


Figure 8. Wear tracks on coatings: (a) Cu coating, and (b) Cu-Bi coating that deposited at 50 mA/cm² for 20 min.

3.5 Electrochemical Analysis

Fig.9 shows the potentiodynamic polarization curves for Cu and Cu-Bi coating in 3.5 wt% NaCl solution. The results of electrochemical measurements obtained from the Tafel plots are presented in Table 2. The average corrosion current density was increased with increasing deposit current density and slightly reduced with the addition of Bi into Cu coating.

The lower current density of the Cu-Bi coating might be attributed to their compact microstructure. Thus, indicating that Cu-Bi deposited at lower current density has a better corrosion resistance than the Cu coating. The similar result was also found in the previous study with the addition of Bi into Zn coating [1]. The corrosion current density reduced from 80 $\mu\text{A}/\text{cm}^2$ to 35 $\mu\text{A}/\text{cm}^2$ with the addition of 0.1 ml Bi electrolyte into common alkaline Zn bath solution. Bi might be act as inert physical barriers to inhibits or slow down the corrosion process [22]. However, deposition at the higher current density, resulted the forming of porous microstructure as shown in Fig. 3 (a3 and b3), and thus caused a higher current density.

Table 2. Electrochemical parameters obtained from Tafel plots.

Sample	Current Density for Electrodeposition (mA/cm^2)	Average Corrosion Potential (V)	Average Corrosion Current Density ($\mu\text{A}/\text{cm}^2$)
Cu	10	-0.206 ± 0.011	3.76 ± 0.93
	50	-0.352 ± 0.006	6.29 ± 3.30
	100	-0.341 ± 0.057	9.68 ± 7.69
Cu-Bi	10	-0.273 ± 0.012	2.89 ± 0.34
	50	-0.429 ± 0.054	5.16 ± 1.79
	100	-0.367 ± 0.033	13.60 ± 6.29

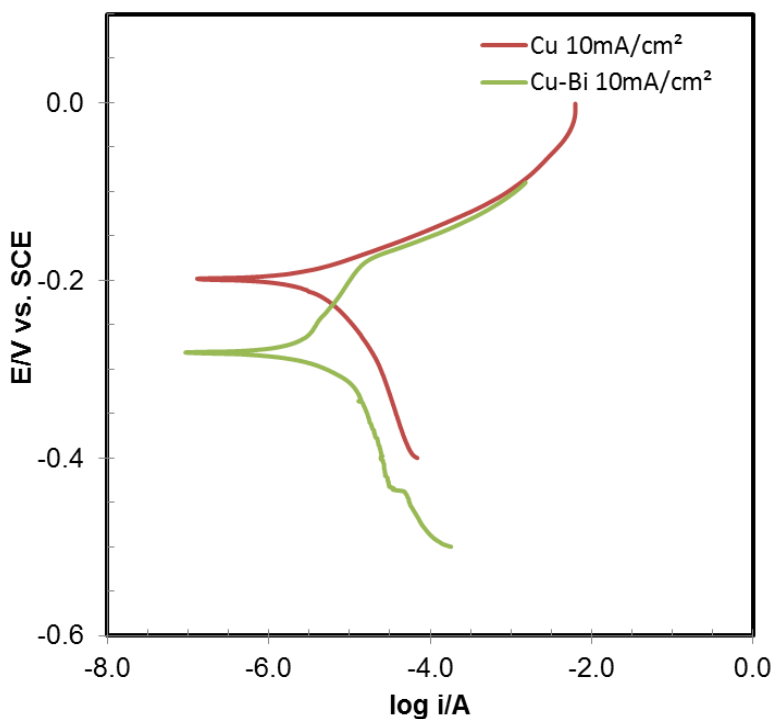


Figure 9. Potentiodynamic polarization curves of Cu and Cu-Bi deposited at 10 mA/cm^2 .

4. CONCLUSIONS

The effects of the incorporation of Bi to the Cu coating on phase structure, microstructure, mechanical properties and electrochemical property were investigated. Based on the experimental results, the following conclusions can be drawn:

- Addition of Bi refined the grains of Cu matrix compared to the pure Cu coating.
- The crystallite size decreased with the increasing deposition current density from 10 mA/cm² to 50 mA/cm². However, the grain size increased with the higher current density, 100 mA/cm².
- The content of Bi deposited into Cu matrix decreased with the increasing deposition current density and shorter deposition time.
- The microhardness increased with deposition current density up to 50 mA/cm² and then decreased at the higher current density. The wear volume loss also increased with the current density.
- Codeposition of Bi slightly enhanced the corrosion resistance measured by electrochemical method. However, deposition at the higher current density reduced the corrosion resistance due to produce of porous microstructure.

ACKNOWLEDGEMENTS

The authors would like to thank the technical staffs and research group members of the Department of Chemical and Materials Engineering, the University of Auckland for their various assistances. See Leng Tay appreciates the financial support from the Bright Spark Unit, University of Malaya.

References

1. W. Chen, L. Wang, W. Gao, *Chem. Eng. J.*, 192 (2012) 242
2. M. Schwartz, Deposition from Aqueous Solutions: An Overview, in: R.F. Bunshah (Ed.) Handbook of Deposition Technologies for Films and Coatings - Science, Technology and Applications (2nd Edition), William Andrew Publishing/Noyes, United States, (1994) 506
3. A.P. Abbott, I. Dalrymple, F. Endres, D.R. MacFarlane, Why use ionic liquids for electrodeposition?, in: F. Endres, A.P. Abbott, D.R. MacFarlane (Eds.) Electrodeposition from Ionic Liquids, Wiley-VCH Verlag GmbH & Co. KGaA, Weinheim, Germany, (2008) 1
4. R. Hauert, J. Patscheider, *Adv. Eng. Mater.*, 2 (2000) 247
5. K.K. Chawla, *Composite Materials: Science and Engineering*, Springer-Verlag, New York (1987)
6. J.R. Ross, J.P. Celis, M.D. Bonte, Electrodeposition of Metals and Alloys, in: R.W. Cahn, P. Haasen, E.J. Kramer (Eds.) Materials Science and Technology: A Comprehensive Treatment, Wiley-VCH Verlag GmbH & Co. KGaA, (2005) 481
7. D. Thiemig, S. Osborne, W. Sweet, J. Talbot, *J. Electrochem. Soc.*, 11 (2008) 35
8. E.J. Podlaha, *Nano Lett.*, 1 (2001) 413
9. V.D. Stankovic, M. Gojo, *Surf. Coat. Technol.*, 81 (1996) 225
10. A. Roldan, E. Gómez, S. Pané, E. Vallés, *J. Appl. Electrochem.*, 37 (2007) 575
11. M. Lekka, D. Koumoulis, N. Kouloumbi, P.L. Bonora, *Electrochim. Acta*, 54 (2009) 2540
12. H. Li, Y. Wan, H. Liang, X. Li, Y. Huang, F. He, *Appl. Surf. Sci.*, 256 (2009) 1614
13. A. Robin, J.C.P. de Santana, A.F. Sartori, *Surf. Coat. Technol.*, 205 (2011) 4596
14. C. Iticescu, G. Cârâc, O. Mitoseriu, T. Lampkt, *Rev. Roum. Chim.*, 53 (2008) 43

15. S.C. Tjong, K.C. Lau, *Mater. Sci. Eng. A-Struct. Mater. Prop. Microstruct. Process.*, 282 (2000) 183
16. Dongming Guo, Min Zhang, Zhuji Jin, R. Kang, *J. Mater. Sci. Technol.*, 22 (2006) 514
17. B. Marković, D. Živković, J. Vřešt'ál, D. Manasijević, D. Minić, N. Talić, J. Stajić-Trošić, R. Todorović, *Calphad.*, 34 (2010) 294
18. X.J. Wei, W.W. Chen, Y.X. Wang, S.L. Tay, W. Gao, *Trans. Nonferrous Met. Soc. China*, 23 (2013) 2939
19. H. Gül, F. Kılıç, S. Aslan, A. Alp, H. Akbulut, *Wear*, 267 (2009) 976
20. B.M. Praveen, T.V. Venkatesha, *Appl. Surf. Sci.*, 254 (2008) 2418
21. A.P.I. Popoola, O.S.I. Fayomi, O.M. Popoola, *Int. J. Electrochem. Sc.*, 7 (2012) 4860
22. P.Q. Dai, Y.H. Zhong, X. Zhou, *Surf. Eng.*, 27 (2011) 71

© 2014 The Authors. Published by ESG (www.electrochemsci.org). This article is an open access article distributed under the terms and conditions of the Creative Commons Attribution license (<http://creativecommons.org/licenses/by/4.0/>).